RSC Advances

ROYAL SOCIETY OF CHEMISTRY

www.rsc.org/advances

The rare earth ruthenium pyrochlore $Ho_2Ru_2O_7(s)$: Thermodynamic properties by electrochemical cell and differential scanning calorimetric measurements

Aparna Banerjee,* A. R. Joshi

Product Development Division, RC & I Group, Bhabha Atomic Research Centre, Mumbai - 400 085,India.

*Corresponding Author

Email: aparnab@barc.gov.in; aparna_baner@yahoo.com (A. Banerjee)

PHONE: +912225593990

FAX: +91-22-25505151

+91-22-25505345

****

Abstract

The Gibbs energy of formation of $Ho_2Ru_2O_7$(s) has been determined employing a solid-state electrochemical cell incorporating an oxide ion conducting electrolyte. The reversible electromotive force (e.m.f.) of the following cell has been measured:

Cell: (-)Pt/{Ho_2O_3(s)+$Ho_2Ru_2O_7$(s)+ Ru(s)}//CSZ// O_2(p(O_2) = 21.21 kPa)/Pt(+)

The Gibbs energy of formation of $Ho_2Ru_2O_7$(s) from elements in their standard state, calculated by the least squares regression analysis of the data obtained in the present study, can be given by:

$$\{\Delta_f G^\circ(Ho_2Ru_2O_7, s) / (kJ\cdot mol^{-1}) \pm 2.6\} = -2518.6 + 0.6225 \cdot (T / K);$$

$$(937 \leq T / K \leq 1265).$$

Standard molar heat capacity $C^\circ_{p,m}(T)$ of $Ho_2Ru_2O_7$(s), was measured using a heat flux type differential scanning calorimeter (DSC) in the temperature range from 307 K to 765 K. The heat capacity was fitted into a mathematical expression and can be represented by:

$$C^\circ_{p,m}((Ho_2Ru_2O_7,s,T)(J\cdot K^{-1}\cdot mol^{-1}) = 289.8 + 3.06 \cdot 10^{-2}T(K) - 33.74 \cdot 10^5/T^2(K).$$

$$(307 \leq T\,(K) \leq 765)$$

The heat capacity data of $Ho_2Ru_2O_7$(s), along with the data obtained from the oxide electrochemical cell were used to calculate the standard enthalpy of formation and absolute molar entropy of the compound.

***Keywords*:** Pyrochlore; Solid-state electrochemical technique; Differential Scanning calorimeter; Thermodynamic Properties; Specific Heat.

1. Introduction

Pyrochlores are technologically important oxides for use in electrochemical devices such as solid oxide fuel cells [1], as components in thick film resistors [2], as well as in thermal barrier coatings [3,4]. The pyrochlores are good refractory materials and have good chemical durability making them prospective candidates for nuclear waste matrices [5,6,7] as also reported for fluorite-type structure [8,9]. The incorporation of plutonium in lanthanum zirconate pyrochlore has been investigated recently by Gregg et al. [10]. Uranium doped zirconium pyrochlores were studied at ambient and high pressure by Zhang et al. [11]. Lutique et al. [12] determined the thermodynamic functions of a few lanthanide zirconate pyrochlores. Pyrochlores are geometrically frustrated magnetic systems exhibiting spin-ice behavior [13,14]. Hence pyrochlores show interesting low temperature properties [15]. Ryzhkin [16] has proposed a theory of magnetic relaxation for the rare earth titanium pyrochlores, $Ho_2Ti_2O_7$, $Dy_2Ti_2O_7$ and $Yb_2Ti_2O_7$ that show spin-ice behavior. Siddharthan et al. [17] carried out theoretical simulations for the rare earth pyrochlore family $R_2Ti_2O_7$ (R=rare earth). The structure and magnetic properties of molybdenum pyrochlores $Y_2Mo_2O_7$ and $Tb_2Mo_2O_7$ were investigated by Reimers et al. that show spin-glass behavior [18,19]. Bramwell et al. attributed the spin ice state to geometric frustration in magnetic pyrochlore materials [20]. Ferroelectricity was observed in the double perovskite $Dy_2Ru_2O_7$ by Xu et al. [21]. Bansal et al. [22] reported crystal structure and carried out magnetic measurements using a Quantun Design SQUID magnetometer in the temperature range from 5 K to 300 K and determined magnetic properties of the pyrochlore $Ho_2Ru_2O_7$. Neutron scattering experiments on $Ho_2Ru_2O_7$ by Weibe et al. [23] revealed two magnetic transitions at T=1.4 K and T = 95 K and concluded that $Ho_2Ru_2O_7$ was not a spin ice. Taira et al. [24] observed a lambda type anomaly in the specific heat versus temperature plot at 94 K and could discern a ferromagnetic transition below 1.8 K. Though structural studies, magnetic measurements and theoretical simulations of a few pyrochlores have been carried out thermodynamic data is scarce. Knowledge about the thermodynamic stability of ruthenium pyrochlores is essential to determine their behavior in various process conditions.

In this study, based on the phase relations, a solid-state electrochemical cell was designed to measure the Gibbs energy of formation of the ternary oxide $Ho_2Ru_2O_7$(s), using

15 mole percent calcia-stabilized- zirconia (CSZ) solid electrolyte, in the temperature range from 937 K to 1265 K. The heat capacity of $Ho_2Ru_2O_7$(s) was measured from 307 K to 765 K using a differential scanning calorimeter (DSC-131, Setaram, France). Other thermodynamic properties were evaluated from these experimental results.

2. Materials and Methods

2.1. Materials

$Ho_2Ru_2O_7$(s) was synthesized from stoichiometric ratios of preheated Ho_2O_3(s) (0.9985 mass fraction, Leico, Industries Inc.) and RuO_2(s) (0.997 mass fraction, Prabhat Chemicals, India). The oxides were intimately ground together in an agate mortar and the mixture was then pelletized. The pellet was made using tungsten carbide die at a pressure of 10 MPa. The pellets were sealed in an evacuated quartz ampoule and heated to T = 1400 K for twenty four hours. Interaction of the sample material with quartz ampoule was prevented by stacking pellets in the ampoule and using the pellet in contact with the quartz as the sacrificial pellet. A few firings at the same temperature with intermediate grindings were necessary till a pure phase was obtained. The formation of the compound was confirmed by X-ray diffractometry. The values of the interplanar spacing d obtained for $Ho_2Ru_2O_7$(s) using STOE diffractometer with Cu-K_α radiation (λ =1.5406 Å) is in good agreement with those reported in JCPDS file number #28-447 [25] and is shown in Fig. 1. Fig.1. includes low intensity peaks attributable to Ho_2O_3(s). The cationic ratio of Ho/Ru of the compound $Ho_2Ru_2O_7$(s) was confirmed to be 1 by energy dispersive X-ray fluorescence (EDXRF).

In the Ho-Ru-O system, the oxides $Ho_2Ru_2O_7$(s) and Ho_3RuO_7(s) [26] have been reported, the former lies on the tie line between Ho_2O_3(s) and RuO_2(s). Phase relations were explored involving different phase mixtures of oxide phases and metal, by equilibration at 1200 K and phase analysis of quenched samples. The phase composition of {Ho_2O_3(s) + $Ho_2Ru_2O_7$(s) + Ru(s)} remained unaltered by equilibration. Hence a phase mixture of {Ho_2O_3(s) + $Ho_2Ru_2O_7$(s) + Ru(s)} in the molar ratio of 1:1:2 was pelletized into a pellet of dimension 10 mm diameter and 3 mm in thickness, using tungsten carbide die at a pressure of 100 MPa and used for e.m.f. measurements.

2.2. The oxide cell assembly

A double compartment cell assembly with 15 mole percent, calcia-stabilized-zirconia (CSZ) solid electrolyte tube with one end closed and flat was used to separate the gaseous

environments of the two electrodes. The dimensions of the CSZ tube used were 13 mm outer diameter, 9 mm inner diameter and 380 mm in length, supplied by Nikatto Corporation Japan. A schematic diagram of the in-house fabricated experimental set-up used and experimental details are described in an earlier publication [27]. Purified argon gas served as the cover gas over the working electrode, in order to achieve a low oxygen potential environment throughout the experiment. Argon gas was passed through towers containing molecular sieves, magnesium perchlorate, the reduced form of BASF catalyst and hot uranium metal. The gas was bubbled out at a steady rate through an oil bubbler without disturbing the equilibrium at the working electrode. A Faraday cage was placed between the furnace and cell assembly and ground to minimize induced electro-motive force (e.m.f.) on the cell leads. Alumina sheathed Pt leads was used to measure the e.m.f. The e.m.f. (±0.1 mV) was measured by a high impedance Keithley 614 electrometer. Synthetic dry air from an air generator was used as the reference electrode. The sample pellet was made by compaction of a mixture of $Ho_2O_3(s)$ + $Ho_2Ru_2O_7(s)$ + Ru(s) at a pressure of 100 MPa. The cell temperature (± 1 K) was measured by a calibrated chromel-alumel thermocouple located in the vicinity of the pellet. E.m.f. was measured after initially equilibrating the galvanic cells at 1000 K for at least 24 h. The following cell configuration was employed in the present study:

Cell: (-)Pt/{$Ho_2O_3(s)$ + $Ho_2Ru_2O_7(s)$ + Ru(s)}//CSZ// $O_2(p(O_2) = 21.21$ kPa)/Pt(+).

The reversibility of the solid-state electrochemical cell was checked by micro-coulometric titration in both directions. The range of permissible oxygen partial pressures for purely ionic conduction for CSZ electrolytes is about 10^{-20} Pa at 1000 K and 10^{-13} Pa at 1273 K [28]. The oxygen partial pressure of the above designed cell falls within this range.

2.3. Measurement of Heat Capacity of $Ho_2Ru_2O_7(s)$:

Heat capacity measurements were carried out using a heat flux type differential scanning calorimeter (Model: DSC-131, Setaram Instrumentation, France). The transducer of DSC-131 has been designed using the technology of the plate shaped DSC rods made of chromel-costantan. It is arranged in a small furnace with a metal resistor of low thermal inertia so as to produce high heating and cooling rates, thereby providing for high speed experiments. The transducer also possesses very good sensitivity over the entire temperature range (100 K to 950 K). The temperature calibration of the calorimeter was

carried out in the present study by the phase transition temperature of National Institute of Standards and Technology (NIST) reference materials (indium: T_{fus} = 429.748 K; tin T_{fus} = 505.078 K; lead: T_{fus} = 600.600 K) and AR grade samples (deionised water: T_{fus} = 273.160 K; potassium nitrate: T_{fus} = 400.850 K; silver sulfate: T_{fus} = 703.150 K; potassium sulfate: T_{fus} = 856.150 K). Heat calibration of the calorimeter was carried out from the enthalpies of transition of the reference materials. For the determination of heat capacity, NIST synthetic sapphire (SRM 720) in the powder form was used as the reference material [29]. Heat capacity of the oxide was determined in the temperature range from 307 K to 765 K.

The classical three-step method in the step heating mode was followed in this study to measure the specific heat in the temperature range under consideration as illustrated in the literature [30]. In the temperature range, from 307 K to 765 K, three sets of experiments were carried out in argon atmosphere at a heating rate of 5 K min^{-1} and a gas flow rate of 2 dm^3 h^{-1}. All the experiments were carried out under identical experimental conditions viz. heating rate, carrier gas flow rate, delay time and temperature range. Two empty, flat bottomed cylindrical aluminium crucibles with covering lids (capacity 10^{-4} dm^3) of identical masses were selected for the sample and reference cells. In the first run both the sample and reference cells were loaded with empty aluminum crucibles. The heat flow versus temperature was measured. In the second run a known weight of NIST synthetic sapphire (SRM-720) was loaded in the sample cell keeping the crucible in the reference side empty and once again the heat flow versus temperature was measured in the same temperature range and at the same heating rate. In the third run, a known weight of the sample was loaded in the sample cell, reference cell being empty and once again the heat flow as a function of temperature was measured. About 300-350 mg of the sample was used for the heat capacity measurements. In DSC-131, heat capacity of the sample under investigation can be calculated by a simple comparison of the heat flow rates in three runs. For a defined step of temperature, the thermal effect corresponding to the sample heating is integrated. Thermal equilibrium of the sample is reached after each step of temperature. If T_i, represents the initial temperature, the temperature interval step is chosen between T_j and T_{j+1}, we define: $T_j = T_i + \Delta T$ and $T_{j+1} = T_i + (j+i)\ \Delta T$. The expression used for the calculation of heat capacity of the sample is given as:

$$C_p(T_i \rightarrow T_{i+1}) = \frac{\int_{Ti}^{Ti+1} HF_{sample}\,dT - \int_{Ti}^{Ti+1} HF_{blank}\,dT}{\int_{Ti}^{Ti+1} HF_{ref}\,dT - \int_{Ti}^{Ti+1} HF_{blank}\,dT} \cdot \frac{Mass_{ref}}{Mass_{sample}} \cdot C_{pref}\,\frac{T_i + T_{i+1}}{2} \qquad (1)$$

where, HF_{blank}, HF_{Ref} and HF_{sample} represent heat flow during first, second and third runs respectively. $C_p(T_j)_{sample}$ and $C_p(T_j)_{Ref}$ represent the heat capacities of sample and reference material in joule per Kelvin per gram and M_{sample} and M_{Ref} represent the mass of sample and reference, respectively. The heat capacity thus obtained was then converted to joule per Kelvin per mole. Accuracy of measurements were checked by measuring the specific heat of Fe_2O_3(s) (mass fraction 0.998) in the temperature range from 300 K to 765 K and the values were found to be within ± 2% as compared with the literature values [31].

3. Results and Discussion

3.1. Solid-State Electrochemical Measurements using oxide cell:

E.m.f. of the solid state oxide electrochemical cell is related to the partial pressure of oxygen at the two electrodes and is given by the relation:

$$E = (RT/nF) \cdot \int_{p'(O_2)}^{p''(O_2)} t(O^{2-}) \cdot \mathrm{d} \ln p(O_2) \qquad (2)$$

E, is the measured e.m.f. of the cell in volts, R = 8.3144 J· K^{-1}· mol^{-1} is the universal gas constant, n is the number of electrons participating in the electrode reaction, F = 96486.4 C·mol^{-1} is the Faraday constant, T is the absolute temperature, $t(O^{2-})$ is the effective transference number of O^{2-} ion for the solid electrolyte and $p''(O_2)$ and $p'(O_2)$ are the equilibrium oxygen partial pressures at the positive and negative electrodes respectively [28]. The transport number of oxygen ion in the present electrolyte cell arrangement is nearly unity ($t(O^{2-}) > 0.99$) at the oxygen pressures and temperatures covered in this study.

Hence, the e.m.f. of the cell is directly proportional to logarithm of the ratio of partial pressures of oxygen at the electrodes:

$$E = (RT / nF) \cdot \ln \{ p''(O_2) / p'(O_2) \}. \quad (3)$$

Thus,

$$nFE = RT \ln p''(O_2) - RT \ln p'(O_2), \quad (4)$$

where, $RT \ln p''(O_2)$ is the oxygen chemical potential over the positive electrode and $RT \ln p'(O_2)$ is the oxygen chemical potential over the negative electrode.

The reversible e.m.f.s of the cell measured as a function of temperature is shown in Fig. 2.

The half-cell reaction at the cathode and the anode for the cell can be given by:

$$2\ O_2(g) + 8\ e^- = 4\ O^{2-}, \quad \text{(at the cathode)} \quad (5)$$

$$Ho_2O_3(s) + 2\ Ru(s) + 4\ O^{2-} = Ho_2Ru_2O_7(s) + 8\ e^-, \quad \text{(at the anode)} \quad (6)$$

The overall cell reaction can be represented by:

$$Ho_2O_3(s) + 2\ Ru(s) + 2\ O_2(g) = Ho_2Ru_2O_7(s), \quad (7)$$

The least square regression analysis of the e.m.f. gives:

$$E / V(\pm 0.0027) = 0.8349 - 5.062 \cdot 10^{-4} \cdot (T / K); \quad (937 \le T / K \le 1265). \quad (8)$$

The uncertainties quoted are the standard deviation in e.m.f. The $\Delta_r G^\circ(T)$ for the reaction given in equation (7) involves the transfer of eight electrons and hence from Nernst equation under conditions of reversible equilibrium we get:

$$\Delta_r G^\circ(T) = -8FE = \Delta_f G^\circ\{Ho_2Ru_2O_7(s)\} - \Delta_f G^\circ\{Ho_2O_3(s)\} - 2\ RT \ln p(O_2). \quad (9)$$

From eqs. (7), (8) and (9) and literature value of $\Delta_f G^\circ\{Ho_2O_3(s)\}$ [32], given by

$$\{\Delta_f G^\circ(Ho_2O_3, s) / (kJ \cdot mol^{-1})\} = -1874.1 + 0.2826 \cdot (T / K) \quad (10)$$

The $\Delta_f G^\circ$ of $Ho_2Ru_2O_7$ (s) has been obtained as:

$$\{\Delta_f G^\circ(Ho_2Ru_2O_7, s) / (kJ \cdot mol^{-1}) \pm 2.6\} = -2518.6 + 0.6225 \cdot (T / K). \quad (11)$$

The error includes the standard deviation in e.m.f. and the uncertainty in the data taken from the literature. The Gibbs energy of formation is a linear function of temperature within the experimental temperature range. The slope and intercept of this linear equation corresponds, respectively, to the average values of the standard molar entropy and enthalpy of formation of $Ho_2Ru_2O_7$(s).

3.2. *Standard Molar Heat Capacity of $Ho_2Ru_2O_7$(s):*

The heat capacity values of $Ho_2Ru_2O_7$(s) were obtained in the temperature range from 307 ≤ *T* (K) ≤ 765, and are given in Table 1 and are taken at 101.325 kPa. The values of heat capacities are best fitted into the following mathematical expression by the least squares method.

$$C^{\circ}_{p,m}(Ho_2Ru_2O_7,s,T)(J\cdot K^{-1}\cdot mol^{-1}) = 289.8 + 3.06\cdot 10^{-2}T(K) - 33.7\cdot 10^{5}/T^{2}(K). \quad (12)$$

The molar heat capacity of $Ho_2Ru_2O_7$(s) at 298.15 K from the above equation was calculated to be 261 $J\cdot K^{-1}\cdot mol^{-1}$. The molar heat capacity at 298.15 K was also estimated in the present study by the Neumann Kopp's rule i.e. from the heat capacity data of the constituent binary oxides. Based on the heat capacity data of RuO_2(s) and Ho_2O_3(s) [33] the estimated heat capacity of $Ho_2Ru_2O_7$(s) at 298.15 K was found to be 227.5 $J\cdot K^{-1}\cdot mol^{-1}$. The heat capacity data for $Ho_2Ru_2O_7$(s) has been reported for the first time.

3.3. Molar Enthalpy of formation and absolute molar entropy:

The molar enthalpy of formation of $Ho_2Ru_2O_7$(s) at 298.15 K has been calculated by the second law method. Heat capacity data obtained in this study by using a differential scanning calorimeter along with transition enthalpies of Ho(s), Ru(s) [28], and O_2(g) [34], were used to determine the second law value of $\Delta_f H_m^{\circ}$ ($Ho_2Ru_2O_7$,s,298.15 K) and was found to be – 2586.8 $kJ\cdot mol^{-1}$. From the heat capacity measurements and the entropy at the average experimental temperature the standard molar entropy S° (298.15 K) for this compound was calculated to be $S^{\circ}_m\{ Ho_2Ru_2O_7,s, 298.15\ K\} = 401.8\ J\cdot K^{-1}\cdot mol^{-1}$. Based on the measured heat capacity, and the estimated entropy, the derived thermodynamic functions of $Ho_2Ru_2O_7$(s) were calculated and the resulting values were extrapolated to 1000 K and are given in Table 2.

4. Conclusion

The pyrochlore $Ho_2Ru_2O_7$(s), an important compound in the field of magnetic materials was synthesized by solid-state reaction route and characterized by X-ray diffraction. In order to predict its stability in various process conditions the Gibbs energy of formation of the ternary compound from elements in their standard state, was determined using solid-state electrochemical oxide cell in the temperature range from 937 K to 1265 K, and found to be: $\{\Delta_f G^{\circ}(Ho_2Ru_2O_7, s) / (kJ\cdot mol^{-1}) \pm 2.6\ \} = -2518.6 + 0.6225\cdot (T / K)$. Only low temperature heat capacity values were reported in the literature, in this

study, the molar heat capacity data for $Ho_2Ru_2O_7(s)$ has been reported at high temperature that is from 307 K to 765 K, and no phase transition could be detected. Complete thermodynamic functions have been generated from heat capacity measurements and Gibbs energy data for the ruthenium pyrochlore $Ho_2Ru_2O_7(s)$.

Acknowledgements:

The authors are grateful to Dr. N. D. Dahale, Fuel Chemistry Division, for X-ray diffraction analysis. The authors are thankful to Dr. K. L. Ramakumar, Director R C & I Group, for his constant support and encouragement.

References:

1. R. G. Edgell, J. B. Goodenough, A. Hamnett, C C Naish, J. Chem. Soc. Faraday Trans., 79 (1983) 893-912.
2. P.F. Careia, A. Ferreti, A. Suna ,J. Appl. Phys., 53 (1982) 5282-5288.
3. R. Vassen, X. Q. Cao, D Basu, D. Stover, J. Am Ceram Soc., 83 (2000) 2023-2028.
4. X. Q. Cao, R. Vassen, W Jungen, S Schwartz, F. Tietz D. Stover, J. Am Ceram Soc., 84 (2001) 2086-2090.
5. R. C. Ewing, Proc. Nucl. Acad. Sci., USA 96 (1999) 3432-3439.
6. S. Lutique, R. J. M. Konnings, V. V. Rondinella, J. Somers, D. Staica, T. Wiss, J. Nucl. Mater., 319 (2003) 59-64.
7. R. C. Ewing, W. J. Weber, F. N. Clinard, Prog. Nucl. Energy., 29 (1995) 635-643.
8. N. K. Kulkarni, S. Sampath, V. Venugopal, Ceramic International, 27 (2001) 839-842.
9. Li Wang, T. Liang, J. Adv. Ceram., 1(3) (2012) 194-203.
10. D. J. Gregg, Y. Zhang, S. C. Middleburgh, S. D. Conradson, G. Triani, G. R. Lumpkin, E. R. Vance, J. Nucl. Mater., 443 (2013) 444-451.
11. F. X. Zhang, M. Lang, C. Tracy, R. C. Ewing, J. Gregg, G. R. Lumpkin, J. Solid State Chem., 219 (2014) 49-54.
12. S. Lutique, P. Javorsky, R. J. M. Konnings,J. C. Krupa, A.C.G. vam Genderen, J.C. van Miltenburg, F. Wastin, J. Chem. Thermodynamics, 36 (2004) 609-618.
13. A. P. Ramirez, A. Hayashi, R. J. Cava, R. Siddharthan, B.S. Shastry, Nature, 399 (1999) 333-335.
14. P. Bonville, J. A. Hodges, M. Ocio, J. P. Sanchez, P. Vulliet, S. Sosin, D. Braithwaite, J. Phys. Condens. Matter, 15 (2003) 7777-7778.
15. A. P. Ramirez, Annu. Rev. Mater. Sci., 24 (1994) 453-480.
16. I. A. Ryzhkin, J. Expt. and Theoretical Phys., 101(3) (2005) 481-486.
17. R. Siddharthan, B. S. Shastry, A. P. Ramirez, A. Hayashi, R. J. Cava, S. Rosenkranz, Phys. Rev. Lett., 83 (9) (1999) 1854-1857.
18. J. N. Reimers, J. E. Greedan, M. Sato, J. Solid State Chem., 72 (1988) 390-394.

19. J. N. Reimers, J. E. Greedan, S. L. Penny, C. V. Stager, J. Appld. Phys., 67 (1990) 5967-5970.
20. S. T. Bramwell, M. J. P. Gingras, Science, 294 (2001) 1495-1501.
21. Z. C. Xu, M. F. Liu, L. Lin, H. Liu, Z. B. Yan, J. M. Liu, Front. Phys. 9 (1) (2014) 82-89.
22. C. Bansal, H. Kawanaka, H. Bando, Y. Nishihara, Phys. Rev., B 66 (2002) 52406(1-4).
23. C. R. Weibe, J. S. Gardner, S. J. Kim, G. M. Luke, A. S. Wills, B. D. Gaulin, J. E. Greedan, L. Swainson, Y. Qiu, C. Y. Jones, Phys Rev. Lett., 93 (2004) 76403 (1-4).
24. N. Taira, M. Wakeshima, Y. Hinatsu, J. Mater. Chem., 12 (2002) 1475-1479.
25. Smith, McCarthy, Penn State Univ., Univ. Park, Pennsylvania, U.S.A., ICDD, Grant-in-Aid Report, (1975).
26. F.P.F. Van Berkel, D.J.W. Ijdo, Mater. Res. Bull., 21 (1986) 1103.
27. A. Banerjee, Z. Singh, V. Venugopal, Solid State Ionics, 180 (2009) 1337-1341.
28. J. N. Pratt. Metall. Trans., 21 A (1990) 1223-1250.
29. R. Sabbah, An Xu-wu, J. S. Chickos, M. L. Planas Leitao, M. V. Roux, L. A. Torres, Thermochim. Acta., 331 (1999) 93-204.
30. G. W. H. Hohne, W.F. Hemminger, H. J. Flammershein, Differential Scanning Calorimetry, 2nd ed., Springer, Berlin, 2003.
31. M. W. Chase, Jr., JANAF Thermochemical Tables, fourth ed. J. Phys. Chem., (monograph no. 91995).
32. FactSage, version 5.3.1, Thermo-Chemical Database Software, Thermfact, GTT Technologies, Germany, 1976-2004.
33. O. Kubachewski, C. B. Alcock, P. J. Spencer, "Materials Thermochemistry", 6th. edn., Pergamon, Oxford, 1993.
34. I. Barin, *Thermochemical Data of Pure Substances*,vols. I and II, third ed., VCH Publishers, New York, (1995).

Table 1: Standard molar heat capacity of $Ho_2Ru_2O_7$(s):

T (K)	$C_{p,m}$ J· K^{-1}·mol^{-1}	T (K)	$C_{p,m}$ J·K^{-1}·mol^{-1}
307.5	263.6	544.8	294.9
326.9	266.3	564.7	295.8
346.4	272.9	584.7	296.8
365.9	276.8	604.6	298.0
385.5	279.5	624.6	299.3
405.3	281.8	644.7	300.9
425.2	284.1	664.7	302.5
445.2	286.5	684.7	304.0
465.1	288.8	704.8	305.0
485.0	290.9	724.9	305.8
504.9	292.5	744.9	306.9
524.8	293.8	765.0	308.0

Table 2: Derived thermodynamic functions of $Ho_2Ru_2O_7$(s):

T (K)	$H°_T$-$H°_{298.15}$ (J· mol^{-1})	$C°_{p,m}$ (J·K^{-1}· mol^{-1})	$S_m°$(T) (J·K^{-1}· mol^{-1})	fef[a] (J·K^{-1}· mol^{-1})
300.0	483.3	261.4	286.2	284.6
350.0	13860.3	272.9	327.4	287.8
400.0	27716.5	280.9	364.4	295.1
450.0	41917.8	286.9	397.9	304.7
500.0	56383.6	291.6	428.4	315.6
550.0	71062.6	295.5	456.3	327.1
600.0	85920.7	298.8	482.2	339.0
650.0	100934.1	301.7	506.2	350.9
700.0	116086.0	304.3	528.7	362.8
750.0	131364.0	306.8	549.8	374.6
800.0	146758.8	309.0	569.6	386.2
850.0	162263.2	311.2	588.4	397.5
900.0	177871.8	313.2	606.3	408.6
950.0	193580.2	315.1	623.3	419.5
1000.0	209384.8	317.0	639.5	430.1

Free energy function (fef[a]) = - $\{G^o(T) - H^o(298.15\ K)\} / T$.

Fig. 1: XRD of $Ho_2Ru_2O_7$(s)

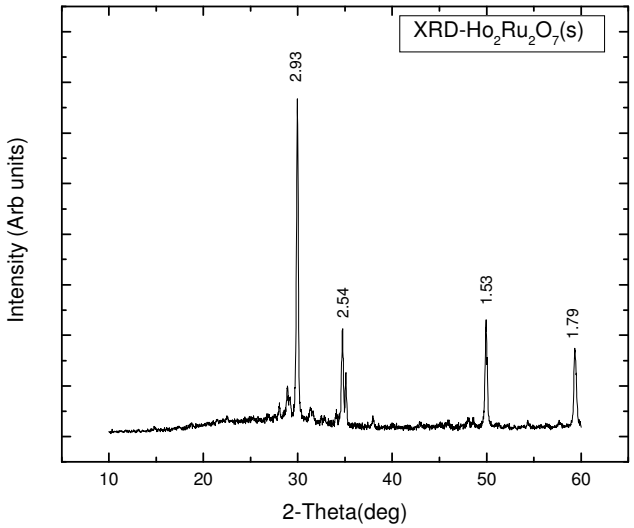

Fig. 2: Plot of e.m.f. as a function of temperature for the cell :

(-)Pt/{$Ho_2Ru_2O_7$(s) + Ho_2O_3(s) + Ru(s)}//CSZ// O_2($p(O_2)$ = 21.21 kPa)/Pt(+).

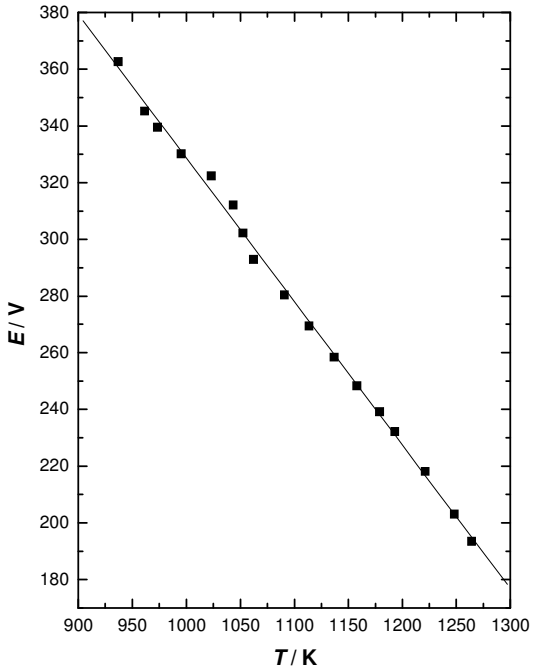

Graphical Abstract

The Gibbs energy of formation of $Ho_2Ru_2O_7$(s) has been determined using a Galvanic cell and employing an oxide ion conducting electrolyte.